in silico Plants, 2026, 8, diag005
https://doi.org/10.1093/insilicoplants/diag005
Published: 2 April 2026
Original Research

Impact of root development, soil texture, and length of the root hair zone on root water uptake

Florian Stoll [1]*, Jan Vanderborght [2], Patrick Duddek [1], Félicien Meunier [3], Adrien Heymans [3,4], Mutez A. Ahmed [5], Andrea Carminati [1]

[1]Department of Environmental System Sciences, ETH Zurich, Universitätsstrasse 16, Zürich 8092, Switzerland
[2]Agrosphere Institute, (IBG-3), Forschungszentrum Jülich, Wilhelm-Johnen-Straße, Jülich, Nordrhein Westfalen 52428, Germany
[3]Earth and Life institute, Université catholique de Louvain, Place Louis Pasteur 3, Louvain-la-Neuve, Walloon Brabant 1348, Belgium
[4]Umeå Plant Science Center, Swedish University of Agricultural Science, Skogsmarksgränd, Umea, Västerbotten County 90736, Sweden
[5]Root-Soil Interaction, TUM School of Life Sciences, Technical University of Munich, Emil-Ramann-Straße, Freising, Bayern 85354, Germany

*Corresponding author. Department of Environmental System Sciences, ETH Zurich, Universitätsstrasse 16, Zürich 8092, Switzerland.
E-mail: florian.stoll@usys.ethz.ch

Abstract

Root hairs are considered to be crucial for facilitating root water uptake, but the specific conditions influencing their impact remain unclear. We present a model that explores the efficacy of root hairs as a function of soil properties, root type, and tissue maturation. In particular, we investigate how the location of root hairs along the root axis, relative to root development, influences root water uptake. The analysis focuses on spatial distribution instead of individual traits such as hair density and length. Using a hydraulic model based on the finite-difference approach, water flow in single maize roots (lateral, seminal, crown, and brace) in two contrasting soil textures (sand and loam) was simulated. Soil water potential, root hair length, and the longitudinal extent of the root hair zone were varied to assess root hair impact on water uptake. (i) Root hairs become increasingly relevant in facilitating root water uptake as soil water potentials decrease. (ii) Root hair effectiveness is greater in sand than loam, due to the lower hydraulic conductivity of sand in the dry range. (iii) In contrast to loam, all root types increase total root water uptake with increasing rhizosphere conductance in sand drier than—2300 hPa. The positive role of hairs in water uptake depends on the profile of root conductivities along the root axis as long as the soil is more conductive than the root. Additionally, root hair functionality depends on soil hydraulic properties and hence is soil texture specific.

Keywords: maize root types, root hair, radial conductance, axial conductance, soil texture, soil conductance

1. Introduction

For decades, plant breeding has focused on high-input agricultural systems, which are often inefficient and heavily reliant on abundant resource availability. This approach came at the cost of reduced root system development, rendering modern crops poorly adapted to changing climatic conditions and resource-limited environments (Lynch 2007, Palta and Watt 2009, Kell 2011, Lynch 2015). With the increasing frequency of droughts and heatwaves affecting croplands (Tripathy et al. 2023, Wang et al. 2023), there is a growing consensus that breeding efforts must prioritize traits that ensure stable and high yields under extreme environmental conditions (Lynch 2015, 2019). One cost-effective trait proposed to enhance drought resilience by improving soil resource acquisition is the development of root hairs (White and Kirkegaard 2010, Brown et al. 2013, Zhang et al. 2018, Marin et al. 2021).

Root hairs are tubular extensions of individual epidermal cells that can absorb water, as indicated in studies using micropotometers, though these approaches have certain methodological caveats (Rosene 1943, Cailloux 1972). By extending into the rhizosphere, root hairs increase the surface area of the root–soil interface, thereby enhancing the hydraulic conductance for water movement from the bulk soil into the root (Peterson and Farquhar 1996, Duddek et al. 2023). This

connection is expected to mitigate dissipation of soil water potential in the rhizosphere and to reduce water flow velocity across this zone. Consequently, given the same potential gradient between xylem and soil water, roots with hairs should exhibit higher water uptake rates than those without, as demonstrated in barley (Carminati et al. 2017). Notably, root hairs were reported to have little effect on shoot hydraulic parameters under wet soil conditions and low evaporative demand (Dodd and Diatloff 2016, Carminati et al. 2017). Instead, their impact became evident when soils dried out or evaporative demand increased (Carminati et al. 2017, Marin et al. 2021, Duddek et al. 2023). The hydraulic role of root hairs is expected to be particularly relevant in coarse-textured soils, where poor root–soil contact and a steeply declining unsaturated hydraulic conductivity curve limits water uptake (Duddek et al. 2023).

An often-overlooked factor in previous studies is the interaction between root hair efficacy and the underlying root demography. Root water uptake and transport capacities change over time (Vetterlein and Doussan 2016). As roots grow, they exhibit a gradient of maturation along their axis, resulting in spatial variation in both root tissue and rhizosphere hydraulic properties. A root pressure experiment by Frensch and Steudle (1989) showed that the first 2 cm of the roots were particularly limited by low axial hydraulic conductance. Root axial conductance is strongly linked to the maturation of the (meta-)xylem vessels, which are not fully matured in the root hair zone (McCully and Canny 1988) impacting the ability of distal segments to take up water (Ahmed et al. 2016). Root radial hydraulic conductance varies longitudinally mainly because of formation of hydrophobic barriers in the apoplast deposited during the maturation of specialized tissue, such as the endo- and exodermis (Peterson 1988, Hose et al. 2001, Enstone et al. 2002). Hydrophobic deposition levels and developmental stages of the endodermis are closely linked to tissue age but have also been shown to depend on water availability, and the growth medium (Zimmermann et al. 2000, Enstone et al. 2002, Lobet et al. 2014). These time-dependent changes create root-type-specific gradients, dividing the root into distinct zones for water absorption and transport (Schneider and Lynch 2018). For instance, Ahmed et al. (2016) found that in 2-week-old maize, lateral roots were primarily responsible for water uptake, whereas seminal roots mainly transported water to the shoot. In a follow-up study on 5-week-old maize, water uptake was dominated by crown roots and their laterals, while seminal roots played a minor role (Ahmed et al. 2018). Interestingly, crown and nodal roots—unlike seminal roots—could absorb water from their distal segments (Ahmed et al. 2018), highlighting a shift in uptake zones as roots age.

Presence of elongated root hairs (root hair zone) marks the transition from the elongation zone to the maturation zone along the root axis (Hochholdinger et al. 2004). Root hairs eventually die off, restricting their presence to younger, distal root segments. Assuming a maximum lifespan of 7 days, and a root growth rate of 2 cm/day, the root hair zone would span ~14 cm. However, lifespan varies widely—from less than a day to over 21 days—depending on drought stress and developmental stage (Cailloux 1972, Xiao et al. 2020). Root hairs and the associated zone are believed to be critical components of the absorptive region. Yet, their effectiveness in water uptake along the root axis and the optimal extent of the root hair zone remain poorly understood—particularly across different root types and soil textures.

Previous water and nutrient uptake models have largely neglected the complex interaction between root hairs and the heterogeneous rhizosphere. As a result, many concluded that root hairs have negligible impact at the single root or root segment scale (Itoh and Barber 1983, Segal et al. 2008, Leitner et al. 2010). However, a recent model by Duddek et al. (2023) demonstrated that the effect of root hairs becomes apparent only when rhizosphere properties are spatially resolved and their distinct hydraulic behaviour is considered. Yet, the modelling approach was computationally too demanding to simulate root water uptake at the root or root system level, where spatiotemporal variation in root hydraulic properties also play a key role.

To overcome this limitation, we developed a simplified root water uptake model to explore how changes in axial and radial hydraulic conductance, driven by root demography, influence root hair efficacy at the single root scale. The presented model is not designed to advance the representation of radial water uptake by root hairs but rather uses a simple but meaningful radial representation of root hairs to investigate whether the effectiveness of root hairs in water uptake depends on the extent of the root hair zone. Additionally, we test whether the optimal root hair zone length differs among four maize root types (laterals, seminal, crown, and brace), with their varying distribution in radial and axial hydraulic properties, in two contrasting soil textures (sand and loam).

2. Material and methods

2.1 Theory

Our model represents a root and its surrounding rhizosphere in a cylindrical geometry with an effective radial hydraulic conductance ($K_{r,s}$ [$cm^3\ s^{-1}\ hPa^{-1}$]) and an effective axial hydraulic conductance (K_x [$cm^3\ s^{-1}\ hPa^{-1}$]). The radial conductance consists of the rhizosphere hydraulic conductance (K_s [$cm^3\ s^{-1}\ hPa^{-1}$]) and the root radial tissue conductance (K_r [$cm^3\ s^{-1}\ hPa^{-1}$]) in series. The geometry of the rhizosphere is a bigger cylinder surrounding the smaller root cylinder geometry. When root hairs are present, the radius of the root cylinder is increased by the root hair length. We assume optimal root hair hydraulic properties and no dissipation of water potential in the root hair zone as modelled by Segal et al. (2008) (Fig. 1). The root radial conductance K_r is the same regardless of the presence of root hairs. This is justified by the dominant resistance of the endodermis to water flow into the stele so that a change of the outer geometry of the root would negligibly affect K_r.

Following the finite difference approach by Doussan et al. (1998) as described in Meunier et al. (2017), we split the root and rhizosphere cylinder along its longitudinal axis into segments of homogenous hydraulic properties. Each segment is axially connected to the previous one by K_x. Radially, K_r and K_s connect each segment to the bulk soil water potential

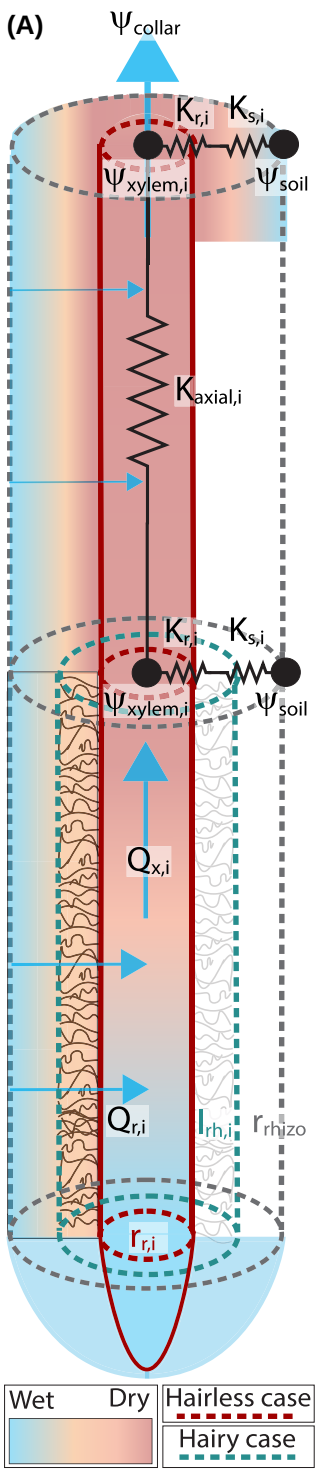

(B) Root process	Function of:	Model input:
Root axial hydraulic conductance: Xylem differentiation	age (distance to root tip)	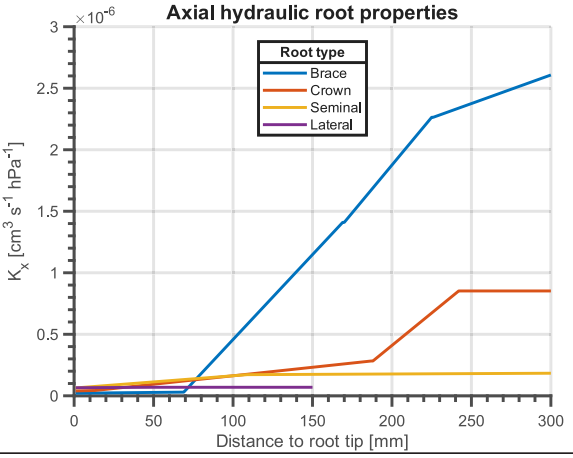
Root radial hydraulic conductance: formation of apoplastic barriers, aquaporins, root cortex decay etc.	age (distance to root tip)	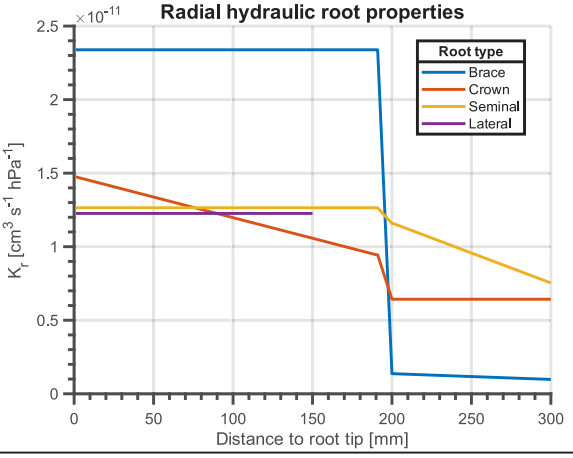
Rhizosphere conductance: root hair length	age (distance to root tip) Ψ_{soil}	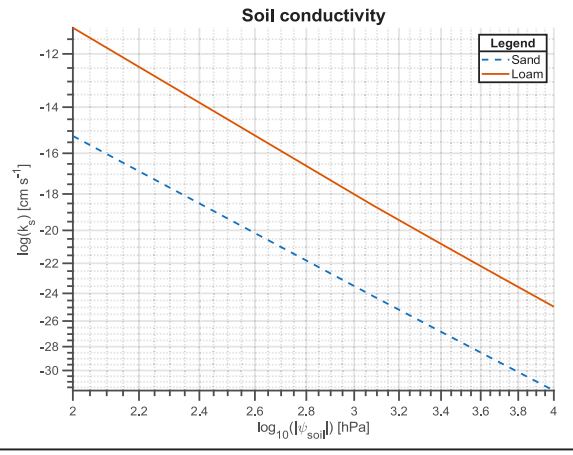

Figure 1 (A) Schematic of a root and its rhizosphere with two axial segments. The lower segment closer to the tip is covered by hairs while the upper segment is bald. The cylinders depicted with dashed lines show the extent of the radial geometries for both the hairy and non-hairy case. The figure is schematic and not drawn to scale. The actual dimensions of each geometry are listed in Table 1. The rhizosphere cylinder (grey, r_{rhizo}), the root hair zone (green, l_{rh}), and the root cylinder (red, $r_{r,i}$). The flow of water is indicated by blue arrows and the water potential is indicated by colour gradients from wet (blue) to dry (red) in non-hairy segments in comparison to hairy segments. The underlying hydraulic architecture in radial and axial directions is shown by pictograms in black. (B) Root and soil processes and their effect on the respective root hydraulic property. The second column shows the main factor influencing the hydraulic property within this process. Other factors that potentially influence the parameter are not considered in this model. First row shows the axial hydraulic conductance (K_x) as a function of distance to the root tip for each root type (Column 3). The distance to the root tip is a proxy for age and cell differentiation and development (Column 2) mainly of the xylem tissue (Column 1). The second row can be read analogous for root radial conductance (K_r). The third row shows rhizosphere hydraulic conductivity k_s as function of soil water potential. To represent the effect of root hairs the rhizosphere conductance (K_s) must be calculated by including the geometry of the root and rhizosphere segment (see Fig. 3).

Table 1. Single Root and rhizosphere model parameters.

Name	Dimension	Range	Description
ψ_s	hPa	$-[10^2:10^4]$	Soil water potential
ψ_x	hPa	$-[10^2:10^4]$	Xylem water potential
ψ_c	hPa	-1.5×10^4	Collar water potential
K_r	$cm^3\,s^{-1}\,hPa^{-1}$	$9.74\times10^{-13}:2.34\times10^{-11}$	Root radial hydraulic conductance
K_x	$cm^3\,s^{-1}\,hPa^{-1}$	$2.14\times10^{-08}:2.61\times10^{-6}$	(Root) Axial hydraulic conductance
K_s	$cm^3\,s^{-1}\,hPa^{-1}$	$2.78\times10^{-15}:4.14\times10^{-6}$	Soil hydraulic conductance
$K_{r,s}$	$cm^3\,s^{-1}\,hPa^{-1}$	$2.79\times10^{-15}:2.34\times10^{-11}$	Radial hydraulic conductance
r_r	cm	0.03 : 0.067	Root radius
rh_{zone}	[–]	–	Root hair zone
r_{rhizo}	cm	1	Rhizosphere radius
l	cm	0.1	Axial root segment length
l_{rh}	cm	0 : 0.04	Axial root hair length
k_0	$[cm\,s^{-1}]$	$6\times10^{-4}:0.048$	Saturated soil hydraulic conductivity
ψ_{soil0}	$[hPa^{-1}]$	$-[29.06:3.402]$	Air entry point
τ	[–]	3:3.6	Tortuosity
Q_r	$cm^3\,s^{-1}$	$1.4\times10^{-11}:3.01\times10^{-7}$	Radial flow
Q_x	$cm^3\,s^{-1}$	$1.4\times10^{-11}:4.23\times10^{-5}$	Axial flow

ψ_{soil} [hPa], which is set as boundary condition. The resulting linear system of equations is rearranged according to the finite-difference solution of water flow in root systems considering mass conservation (Meunier et al. 2017). This allows to solve for the xylem water potential ψ_x [hPa] and the water flow along the radial Q_r [$cm^3\,s^{-1}$] and axial pathway Q_x [$cm^3\,s^{-1}$] of each root segment (see Supplementary Section 12).

Input vector K_x was estimated based on an experiment by Meunier et al. (2018), who used a root pressure probe to measure the axial hydraulic conductance of root segments of variable length (Frensch and Steudle 1989, Meunier et al. 2018). For a detailed explanation of the root pressure probe, see Fig. 1 and text in Frensch and Steudle (1989). The axial conductance k_x[$10^{-4}\,cm^4\,hPa^{-1}d^{-1}$] was divided by the selected segment length l [cm] to obtain the input vector K_x:

$$K_x = \frac{k_x}{l}. \tag{1}$$

Measurements of k_x allowed Meunier et al. (2018) to estimate the root radial hydraulic conductivity k_r [$cm\,hPa^{-1}d^{-1}$] by inversely fitting the water flow through root segments using a piecewise linear function. By additionally accounting for the cylindrical geometry of the root segments, we obtain the input vector K_r:

$$K_r = 2\pi\, r_r\, l\, k_r, \tag{2}$$

where r_r [cm] is the root radius; l is the segment length. The rhizosphere conductance was estimated in several steps. The soil hydraulic conductance was first calculated using the Brooks–Corey model and assuming steady-state conditions and uniform conductivity along the flow pathway from the bulk soil to the root surface. The solution is given by the equation:

$$K_s = \frac{2\pi l}{\log\left(\frac{r_{rhizo}}{r_r + l_{rh}}\right)} k_0 \left(\frac{\psi_s}{\psi_{s,0}}\right)^{-\tau}, \tag{3}$$

where l is the segment length, r_{rhizo} is the rhizosphere radius, k_0 [$cm\,s^{-1}$] is the saturated hydraulic conductivity, ψ_s is the soil water potential, $\psi_{s,0}$ [cm^{-1}] is the air entry value, and τ[–] is the tortuosity in the flow path of the soil water. Brooks–Corey parameters were obtained from Cai et al. (2021), who fitted them to van Genuchten parameters reported by Vetterlein et al. (2021) for loamy and sandy soil types. Note that the root pressure probe experiment by Meunier et al. (2018) was done on roots grown in sandy soil, not in loam.

For comparison and validation, we further calculated the rhizosphere conductance under steady-rate assumption on a segment scale instead of steady state. The radial flux can be represented using the same parameters as in Equation 3 and the water potential at the soil:root interface $\psi_{r,s}$ as follows:

$$Q_r = \frac{2\pi(r_r + l_{rh})l \cdot \frac{k_0}{1-\tau} \cdot \psi_{s,0}^{-\tau} \cdot |\psi_s^{1-\tau} - \psi_{r,s}^{1-\tau}|}{\left(\frac{r_r + l_{rh}}{2} - \frac{(r_r + l_{rh})r_{rhizo}^2(\log(r_{rhizo}) - \log(r_r + l_{rh}))}{r_{rhizo}^2 - (r_r + l_{rh})^2}\right)}. \tag{4}$$

Now, we can calculate the rhizosphere hydraulic K_s conductance under steady rate as follows:

$$K_s = \frac{Q_r}{|\psi_s - \psi_{r,s}|}. \tag{5}$$

Note that K_s under steady rate assumption was not used for model parametrization but only to compare the impact of steady rate versus steady state assumption on K_s.

2.2 Model simulations

The boundary condition ψ_s was varied from −100 to -10^4 hPa in increments of 1100 hPa, resulting in 10 distinct soil drying scenarios. The second boundary condition, the water potential

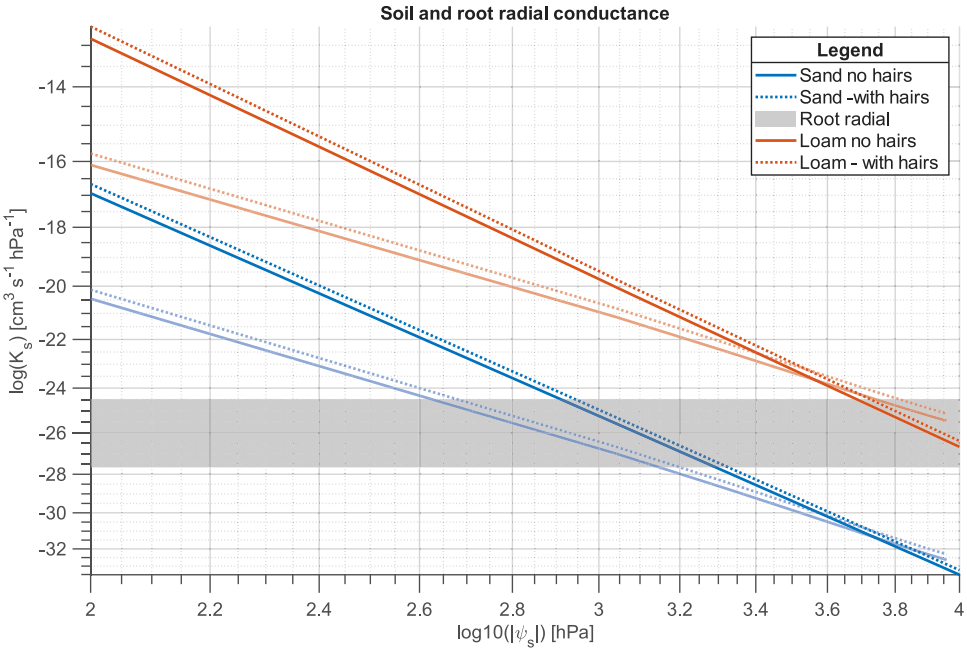

Figure 2 Rhizosphere hydraulic conductance (K_s) as function of soil water potential (ψ_s) for a lateral root segment with and without hairs. Solid lines indicates K_s without root hairs. Dashed lines indicate K_s with root hairs. Non-shaded lines indicate steady state assumption (Equation 3) whereas the transparent lines indicate K_s under steady rate assumption, which was not used for parametrization of this model (Equations 4 and 5). The grey area indicates the range of root radial conductance (K_r) which is also shown in Table 1.

at the root collar ψ_c [hPa], was held constant at $-1.5 \cdot 10^4$ hPa across all scenarios.

Each of the 10 soil drying scenarios was simulated for two soil textures: sandy and loamy soil. This was achieved by adjusting the Brooks and Corey parameters specific to each soil type, including k_0, $\psi_{soil,0}$, and τ.

Additionally, all scenarios were tested for four different root types: brace, crown, seminal, and lateral roots. For each root type, the model was parameterized with type-specific vectors of k_x, k_r, and r_r.

To investigate the role of root hairs, all scenarios were simulated with root hair lengths of $l_{rh} = 0$ and $l_{rh} = 0.04$ cm. For the latter, we also performed simulations with a stepwise increase in the number of root segments bearing root hairs. Specifically, we simulated a stepwise expansion of the root hair zone by first assigning a root hair length of 0.04 cm to only the first root segment, then to the first two segments, then the first three, and so on, cumulatively until the entire root axis was covered. In total, this resulted in $10 \times 2 \times 4 \times 300$ unique simulations, capturing the dimensions of soil drying intensity, soil texture, root type, and root hair zone extent.

2.3 Analysis

Each simulation produced output vectors for Q_r, K_s, $K_{r,s}$, and Q_x. The effect of root hairs, soil type, and root type on total root water uptake was assessed using Q_x from the most proximal xylem segment. The relative increase in water uptake due to root hairs was calculated as:

$$\Delta Q_x = \frac{Q_{x,\text{hair}} - Q_x}{Q_x} \tag{6}$$

where $Q_{x,\text{hair}}$ is the total water uptake in simulations with $l_{rh} = 0.04$ cm for segments 1 through i, and Q_x corresponds to the case where $l_{rh} = 0$ cm for all segments (Fig. 4).

Similarly, the relative increase in K_s was computed as:

$$\Delta K_s = \frac{K_{s,\text{hair}} - K_s}{K_s} \tag{7}$$

where $K_{s,\text{hair}}$ represents the sum of K_s with $l_{rh} = 0.04$ cm for segments 1 through i, and K_s corresponds to the case with $l_{rh} = 0$ cm across all segments (Fig. 5).

We further calculated the local efficiency of root hairs at a given segment as the ratio of ΔQ_x to ΔK_s (Fig. 5).

Moreover, we examined the local impact of root hairs at the segment scale under both steady-state and steady-rate assumptions for loamy and sandy soils (Fig. 2). A separate analysis was conducted along the root axis for each root type in both soil textures (Fig. 3).

3. Results

The estimated rhizosphere hydraulic conductance K_s follows the texture-dependent k_s curves: they are around four orders of magnitude higher in loam than in sand; the slope of k_s and of K_s (steady state approach) are the same in the log scale, and are equal to $\tau = 3$ in loam and $\tau = 3.6$ in sand (Figs. 1 and 2). Root type influences K_s, as it determines the inner rhizosphere radius, which equals the root radius. This is analogous to the geometric effect of root hairs on K_s, as they increase the inner rhizosphere radius by 0.04 cm across all root types. The effect of root hairs on K_s is purely geometric and therefore depends exclusively on the inner and outer rhizosphere radius. As a result K_s increases by 17, 19, 22, and 24% under steady

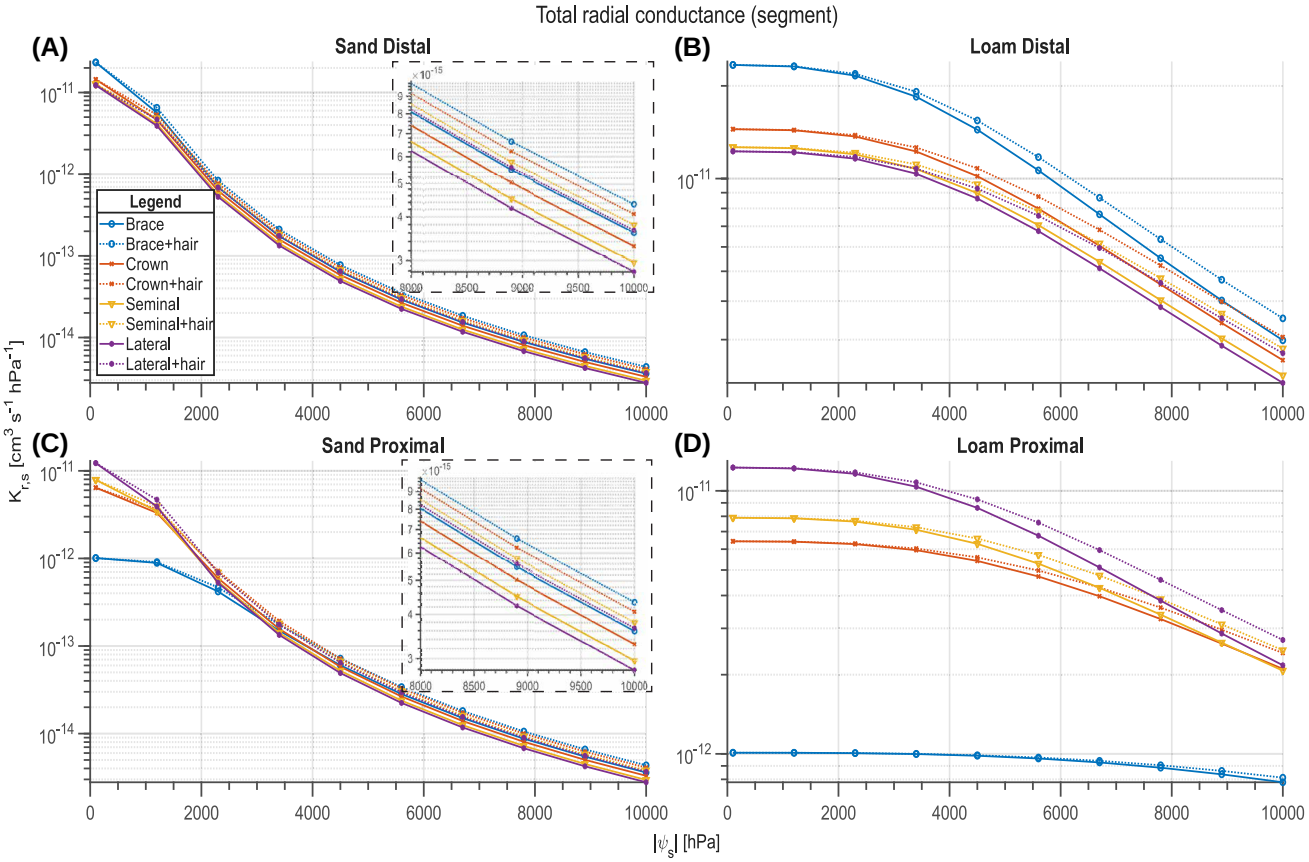

Figure 3 Radial hydraulic conductance ($K_{r,s}(\psi_s)$) for each root type in sand and loam at 1 cm from the root tip (upper two plots) and 1 cm from the root collar (lower two plots). Circles, crosses, diamonds, and asterisks indicate brace, crown, seminal, and lateral root types, respectively. The solid line shows $K_{r,s}$ without hairs, the dashed lines shows $K_{r,s}$ if root hairs are added as an increased inner rhizosphere radius. The positive relative deviation of $K_{r,s}$ when root hairs are added increases with increasing absolute soil water potential (ψ_s).

state assumptions and by 20, 23, 26, and 28% under steady rate assumption for brace, crown, seminal, and lateral root, respectively when the respective root radius is increased by 0.04 cm.

The input parameter K_s spans the greatest range of values, covering over 8 and 7 orders of magnitude within the simulated ψ_{soil} for sand and loam, respectively. It intersects the range of K_r values (Fig. 2) at ~−800 and −5000 hPa and falls below K_r for any value <−2000 hPa in sand. Water fluxes above these values are strongly controlled by subsequent resistances, whereas at lower soil water potentials, K_s imposes the dominant resistance to water fluxes. This pattern is also reflected in Fig. 3, which shows the combined hydraulic conductance of K_s and K_r in series, $K_{r,s}$, across the simulated range of ψ_s. Root type-specific differences are prominent at high soil water potentials, but they decrease to levels comparable to those caused by differences in rhizosphere geometry at lower potentials (Fig. 3, zoom-in). The effect of root hairs on $K_{r,s}$ increases with decreasing soil water potential and is nearly identical across all root types in dry sand. In loam, the effect is stronger in distal segments for all root types except laterals, where it remains the same across both segments. In sand at soil water potentials above −800 hPa, and in loam, the segment conductance $K_{r,s}$ reflects the ranking of subsequent conductance K_r: brace > crown > seminal > lateral in distal segments, and lateral > seminal > crown > brace in proximal segments. In sand with ψ_s below −2000 hPa, the influence of root type is reduced to differences in root radius, following the order: brace > crown > seminal > lateral. This relationship persists also when root hairs are added (Fig. 3).

The increase in $K_{r,s}$ due to the presence of root hairs becomes more pronounced for decreasing soil water potentials. Our model revealed that the relative increase in total root water uptake rate exhibits two distinct patterns: one for wet sand and loam (where $K_s > K_r$), and another for dry sand (where $K_s < K_r$). Figure 4 presents the relative total root water uptake as a function of increasing longitudinal extent of the root hair zone. The efficacy of root hairs is higher in sand than in loam at the same ψ_s. In wet sand and in loam, the relative increase in total root water uptake with increasing root hair zone extent shows a stronger efficacy towards proximal segments in seminal and lateral roots (Fig. 4C, D, G, and H). This is also true for distal segments of brace and crown roots up to 20 and 15 cm, respectively, where the efficacy begins to plateau and is only increasing slightly for brace roots and at a reduced rate for crown roots (Fig. 4A, B, E, and F). In dry sand, increasing the longitudinal extent of the root hair zone induces a proportional increase in total relative root water uptake. The magnitude of this increase follows the inverse order of root radius and is directly related to the total

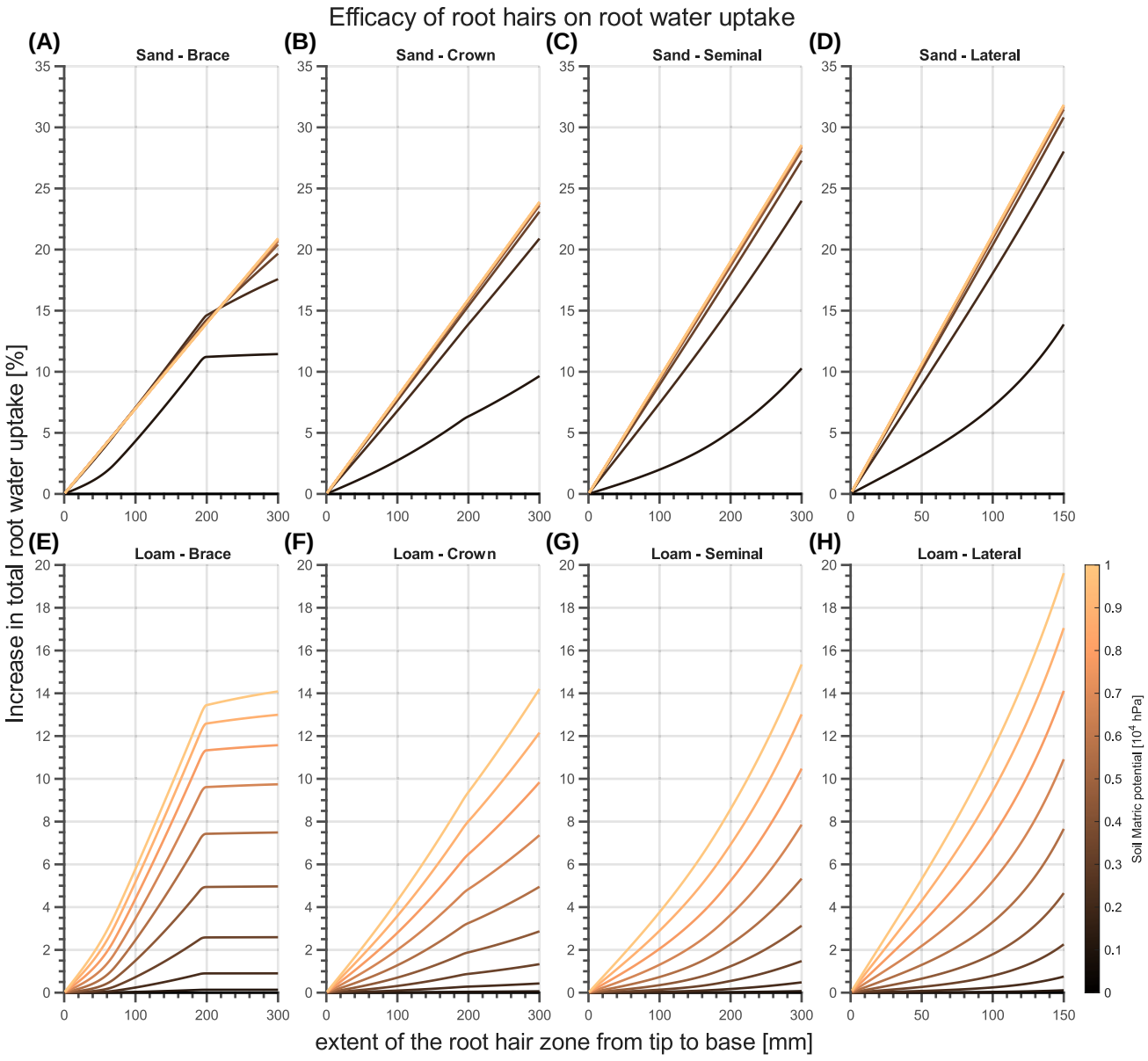

Figure 4 Lines show the trajectory of additional relative total root water uptake (ΔQ_x Equation 6) on the *y*-axis for a given soil water potential (ψ_s) as a function of the longitudinal extent of the root hair zone on the *x*-axis. The first row for sand, the second row for loam. ψ_s is indicated by the colour of the line according to the colourbar on the bottom right in 10^4 hPa. The slope of each line indicates the local increase in efficacy upon an incremental increase in the extent of the root hair zone or soil hydraulic conductance (K_s). The slope of the lines further indicates limitation of root hair efficacy by root axial hydraulic conductance K_x, where it is increasing along its trajectory; limitation by root radial hydraulic conductance K_r where it is decreasing along its trajectory; and no limitation of efficacy when it is along a linear trajectory for the ψ_s.

conductance increase caused by changes in the inner rhizosphere radius for each root type. This relationship is illustrated in Fig. 5A–D, which shows the relative total increase in root water uptake rate as a function of ΔK_s, itself proportional to the increasing extent of the root hair zone. Moreover, it highlights the underlying hydraulic limitations on root water uptake. A linear increase (derivative = 1, Fig. 5E–H) indicates that root water uptake was limited purely by K_s, as observed in sand at ψ_s below 3100 hPa. An increase smaller than 1 suggests that either K_r or K_x limited root water uptake. This was the case in wet sand and loam, where K_s exceeded either K_r or K_x. Limitation by K_x is associated to an accelerating increase, as seen in seminal and lateral roots (Fig. 5G and H), whereas limitation by K_r is associated to a decelerating increase, as observed in distal segments of brace roots beyond 20 cm from the root tip, or proximal segments of crown roots beyond 15 cm from the root tip (Fig. 5E and F). Brace roots even displayed an efficacy considerably >1 in distal parts until 20 cm distance from the root tip for soil water potentials smaller than −2300 hPa. At soil water potentials smaller than −4500 hPa the efficacy reduces to 1 along the entire root axis. This peak in efficacy coincides with K_s within the range of K_r and absence of limitation by K_x (see Section 4. and Fig. 1 in Supplementary).

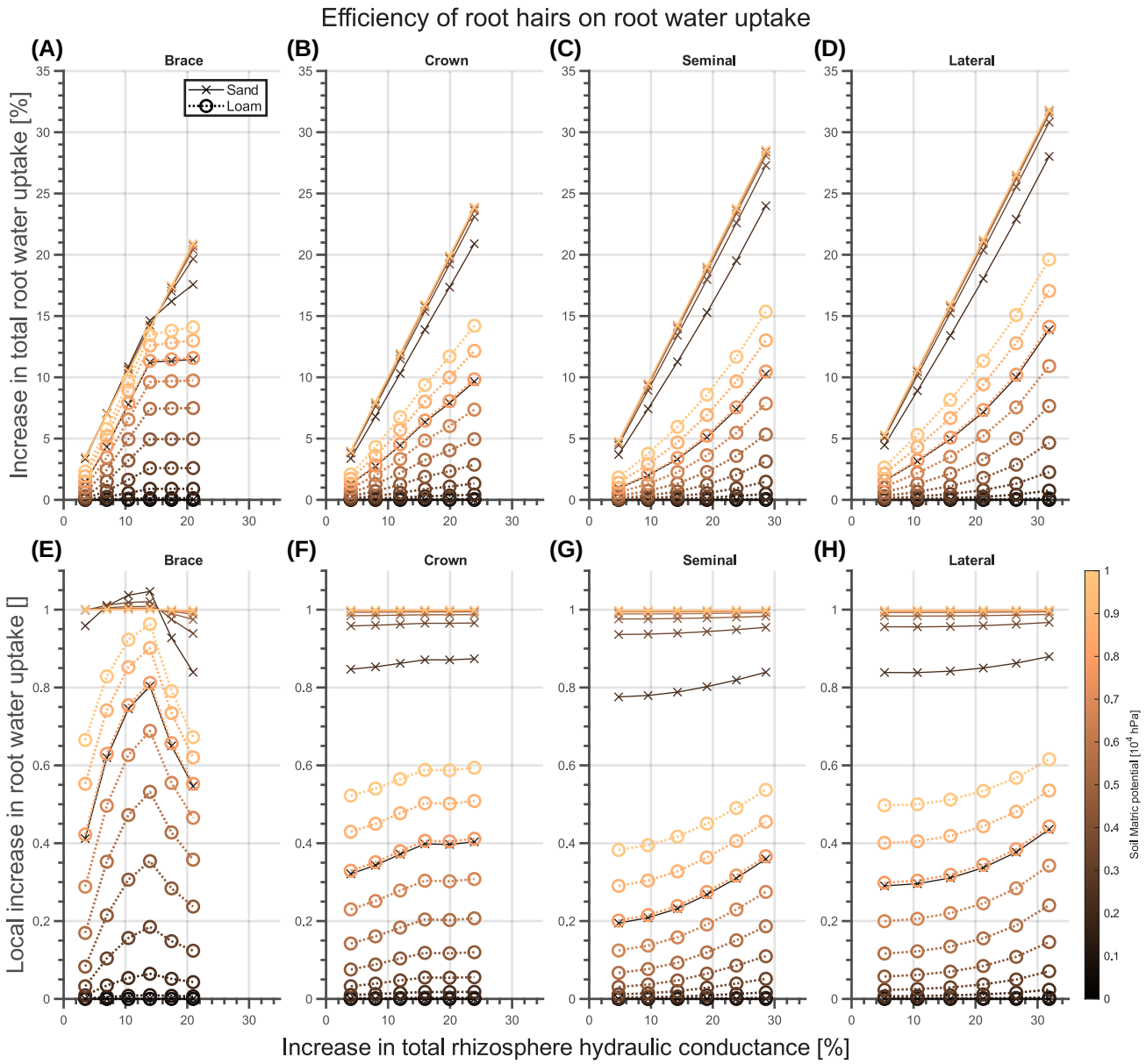

Figure 5 The first row shows the difference in rhizosphere hydraulic conductance (ΔK_s) on the *x*-axis (Equation 7. The increase in the extent of the root hair zone correlates linearly with ΔK_s. Thus, the *x*-axis can be directly related to Fig. 4 for each respective root type. The second row shows the first derivative of the first row. The incremental relative increase of total root water uptake for the respective incremental change in rhizosphere hydraulic conductance (K_s) (*y*-axis) plotted over ΔK_s (*x*-axis). For example, a value approximating 1 means that an increase in K_s is translated 1 to 1 to an increase in total root water uptake. A value of 0 means that the increase in K_s has no effect on total root water uptake. Crosses indicate sand, circles indicate loam, and the colours indicate the respective soil water potential according to the colourbar on the bottom right in 10^4 hPa.

4. Discussion

The simulations show that root hairs can attenuate the limitation imposed on root water uptake by low rhizosphere hydraulic conductance during soil drying on the single root level. All investigated root types display a hydraulic architecture that enables them to profit from this increase in rhizosphere conductance. Rather than root type its the soil texture that governs root hair efficacy. Once the soil is dry in the coarse-textured case the mere presence of root hairs anywhere along the root axis is highly efficient, meaning that root water uptake increases linearly with the increase in rhizosphere conductance induced by root hairs. Root type and underlying tissue maturity are relevant in relatively wet conditions in sand and for all simulated soil water potentials in loam. In these cases, increasing root water uptake rates are limited by low axial conductance for seminal and lateral roots, and they are strongly limited by low radial conductance in proximal segments of brace roots and marginally limited by low radial conductance in proximal segments of crown roots.

4.1 Interaction of root hairs and soil texture

Interestingly, the model showed that under dry conditions the difference in $K_{r,s}$ between the four root types was reduced to their root type specific differences of rhizosphere geometry, because the inner rhizosphere radius equals the root radius, while the outer rhizosphere radius was kept constant. Thus, the pathway through the soil was reduced in its length and the root:soil interface which represents the smallest soil surface area along this pathway was increased by a smaller ratio in bigger roots than in smaller roots. This ratio is also leading to the root type specific geometric factors reported for steady rate and steady state assumptions (see Section 3.). Even though this is only a soil limitation, the magnitude of this geometric effect is displayed by comparing $K_{r,s}$ of the four root types in Fig. 3A and C (zoom in) and when comparing the respective root type with and without hairs. Because K_s rapidly subceeds K_r by 2 orders of magnitude, virtually imposing the sole resistance to root water uptake. This dominant limitation by K_s is already reached in sand at a soil water content of 0.074 $cm^3\ cm^{-3}$, which shows the high likelihood for roots to experience these water potentials under realistic growing conditions. In loam, the limitation by K_s is less drastic and resulted in a co-limitation of K_r, K_x, and K_s, because K_s never dropped below the range of K_r and K_x but reached comparable values. This is indicating a higher relevance of root hairs for root water uptake in coarse-textured soils than in fine-textured soils. Potentially, this interaction of root hair efficacy with soil texture could explain the seemingly contradictory findings on the significance of root hairs for water uptake (Segal et al. 2008, Li et al. 2014, Dodd and Diatloff 2016, Carminati et al. 2017, Cai et al. 2021, Marin et al. 2021, Suzuki et al. 2003). A recent finding by Duddek et al. (2024) suggests that root hairs emerge and elongate preferentially where soil water potentials are low and initial soil root contact is low. As a result, root hair density is expected to be lower in the fine-textured soil in comparison to the coarse-textured soil. Thus, the low efficacy of root hairs in fine-textured soil might manifest at the plant level in an even more pronounced way. On the other hand, in a fine textured but structured soil where initial root:soil contact is low and hairs can bridge the gap between soil and root (Robbins and Dinneny 2015) root hairs are likely to have an effect on root water uptake.

4.2 Interaction of root hairs and root development

Overall, brace roots exhibit the greatest capacity to benefit from root hairs among all the root types investigated—particularly in their distal regions—while showing a reduced benefit in the proximal parts. This is due to their high axial conductance along the root axis. In contrast, the proximal regions of brace roots are constrained by low radial conductance.

Crown roots follow a similar pattern to brace roots, though less pronounced, resulting in a nearly linear efficacy. Seminal and lateral roots, however, are limited by low axial conductance in loamy soils. The maximum efficacy of root hairs is observed at 15 cm from the tip for brace, crown, and lateral roots, and at 30 cm for seminal roots.

Crown and brace roots benefit the most from root hairs and have also been identified as dominant contributors to water uptake in maize of comparable age (Ahmed et al. 2018). These root types also transmit more xylem tension because they are directly connected to the shoot xylem. In doing so, they can even isolate embryonic root types from xylem tension propagation (see Ahmed et al. 2018). This contributes to the low water uptake observed in the unbranched distal parts of seminal roots (Ahmed et al. 2016). However, this behaviour is not reflected in the model used here, as the comparison focuses on the relative efficacy and efficiency at the level of individual root types. Additionally, the variation in root hair efficacy between root types is minor compared to the differences observed between soil types and only present in wet sand and loam.

4.3 Model limitations

This model assumes no differences in the hydraulic properties of the rhizosphere and bulk soil. Previous studies, however, have shown that the hydraulic properties of the rhizosphere are different to those of the bulk soil (Hinsinger et al. 2009, Carminati et al. 2010). Mucilage and the small-scale heterogeneity of the rhizosphere, including cracks and macropores, are not reflected in this model. Additionally, it does not include the preferential root growth along pathways with higher soil porosity. As a result, a root growing in a coarse-textured rhizosphere is characterized by low root:soil contact of the root cylinder which is often non-uniform along the axis and is not captured in our model which assumes uniform ψ_s along the entire root axis. A modelling study by de Willigen et al. (2018) found that roots with partial longitudinal root:soil contact reduced the time that they were able to maintain the shoot water demand. This reduction in time was proportional to the loss in contact when the remaining root:soil contact was asymmetric radial contact but more than proportional if the loss of contact resulted in asymmetric contact along the root axis. Thus root hairs are relatively more effective in a coarse-textured soil because they contribute to a higher fraction of the total root:soil contact and preferentially increase root:soil contact where it is initially low. Based on these arguments, our model is likely to underestimate the relative contribution of root hairs to water uptake. On the other hand, root hairs were represented as an effective increase of the inner rhizosphere radius. Which implies infinite conductivity in the root hair zone. However, pore-scale modelling by Duddek et al. (2023) demonstrates that root hairs primarily linearize the soil water potential dissipation near the root. Therefore, our model represents an optimal scenario, assuming maximum possible root hair efficacy on the segment scale.

Additionally, root hair density was observed to drop exponentially as a function of root–soil contact for example in wheat (White and Kirkegaard 2010). This is not captured in this model since root hairs were presented the same in both soil type scenarios. Additionally, root hair shrinkage was not considered in this model but might reduce the efficacy of root hairs especially in the dry range (Duddek et al. 2022).

Estimation of K_s based on the steady state assumption and uniform K_s was chosen to simulate the uptake along roots because it can be easily built into a linear matrix which can be solved at low computational cost. In contrary, the steady rate assumption results in a non-linear relation between fluxes and potential gradients and would require a more complex and iterative solution. While the effect of root hairs in this model is

purely geometrical it is the same in relative proportions under steady rate and steady state assumption. Differences in K_s mainly occurs in the wet range where ψ_s is bigger than −3500 hPa (Fig. 2). Thus, in the range where K_s is not the dominant resistance.

The parameterization of our model is based on measurements of K_x and subsequent fitting of K_r (Meunier et al. 2018). However, in these experiments the authors grew plants under well-watered conditions (Meunier et al. 2018). As the root hydraulic properties are plastic to water availability, we are aware that the parametrization of our model would have been different if the experiments were conducted under dry soil conditions. Roots respond to soil water stress by decreasing K_r namely by increasing and accelerating suberin deposition (Martre et al. 2001, North et al. 2004, Hachez et al. 2012, Barrios-Masias et al. 2015). Meunier et al. (2018) state that the growing conditions might have been the reason that no variation of k_r was observed for lateral roots in the pressure probe experiments. The decline in k_r of brace roots in the study by Meunier et al. (2018) was likely caused by aerenchyma formation, and fully suberized exo- and endodermis, with tertiary thickening of the endodermis which are processes that correlate with a decline in water uptake of cereal roots (Sanderson 1983, Enstone et al. 2002). Similar processes do not occur in laterals but might have been avoided in other root types because of the well-watered growth conditions. Thus, it is likely that this model underestimates the degree of hydraulic limitation by K_r. Simultaneously, the degree of limitation by K_x is likely overestimated by this model as an indirect effect of overestimation of K_r. But also because of the uniform boundary condition ψ_c which is expected to decrease with increasing branching order and depending on the root–shoot junction conductivity Meunier et al. (2018). Another factor that was not considered in this model is the short-term variability of the symplast hydraulic conductance induced by varying aquaporin activity (Javot and Maurel 2002, Bramley et al. 2009, Caldeira et al. 2014, Chaumont and Tyerman 2014). Conductance of the symplast increases where water is more readily available which would theoretically be in the region of root hairs. Since it is necessary to dissect the roots to measure its permeability in a root pressure probe, there is also an uncertainty to by how much the aquaporin activity was already reduced as speculated by Gambetta et al. (2017).

5. Conclusion and outlooks

The high efficiency of root hairs in water uptake derives from an increase of hydraulic conductance at a hydraulic (and geometric) bottleneck in the rhizosphere domain. The rhizosphere itself represents a hydraulic bottleneck to root water uptake as soon K_s drops below K_r upon soil drying; making root hairs particularly effective in coarse-textured soil. In a fine-textured or wet coarse-textured soils, root hairs are more effective in regions of a root with a high K_r and absence of limitation by K_x.

Our results indicate that the extent of the root hair zone or the longevity of root hairs is an important property to consider when investigating the hydraulic efficacy of root hairs. Root hair lifespan has to be considered in a coordinated system of other age related processes like root cortical senescence, aerenchyma formation, formation of endodermis and exodermis and xylem maturation. Regarding the different root types, the presented model indicates that it is more effective for a plant to increase the extent of the root hair zone in absorptive regions of the root. It is less effective to increase the extent of the root hair zone into transport regions of crown roots and brace roots. This also indicates that the mere presence of root hairs does not ensure their hydraulic efficacy because it can be dependent on underlying root tissue conductance and surrounding rhizosphere hydraulic properties. This has likely masked the hydraulic effect of root hairs for many experimental set ups.

The presented model allows to investigate the efficacy of root hairs in water uptake for different root types. The image-based model pipeline of GRANAR and MECHA (Heymans et al. 2021) could be used to generate hydraulic root anatomies for parametrization of the model and further investigate the interaction of demographic processes with the contribution of root hair water uptake on the root or at the root system scale. This would enable the identification of ideal root anatomy for each soil type and subcellular hydraulic root traits for low input agricultural systems and identification of climate resilient crop varieties (Yu et al. 2024).

Acknowledgments

The authors acknowledge the use of Chat GPT from OpenAI in generating text for this study.

Author contributions

Florian Stoll (Conceptualization, Methodology, Formal Analysis, Writing—Original Draft), Patrick Duddek (Writing—Review and Editing, Visualization), Félicien Meunier (Methodology, Writing—Review and Editing), Adrien Heymans (Methodology, Writing—Review and Editing), Jan Vanderborght (Methodology, Writing—Review and Editing), Mutez Ahmed (Funding Acquisition, Writing—Review and Editing), and Andrea Carminati (Conceptualization, Methodology, Writing—Review and Editing, Funding acquisition)

Supplementary material

Supplementary material is available at *in silico Plants* online.

Conflicts of interest

The authors declare no conflicts of interest.

Funding

This study was supported by German Research Foundation (DFG), project numbers 403670197 ‘Emerging effects of root hairs and mucilage on plant scale soil water relations’ to M.A.A. and J.V. This work was also financially supported by the Kempe Foundation grants JCK-2130 to (A.H.) and F.M. was funded by the Research Foundation -Flanders (FWO) as a senior postdoc and is thankful to this organization for its financial support (FWO grant no. 1214723N).

Data availability

The MATLAB code and data underlying this article are available on Zenodo at https://doi.org/10.5281/zenodo.19225076 and on GitHub at https://github.com/FlowSto/SingleRoot_Model/releases/tag/v1.0.0.

References

Ahmed MA, Zarebanadkouki M, Kaestner A *et al.* Measurements of water uptake of maize roots: the key function of lateral roots. *Plant Soil* 2016;**398**:59–77. https://doi.org/10.1007/s11104-015-2639-6

Ahmed MA, Zarebanadkouki M, Meunier F *et al.* Root type matters: measurement of water uptake by seminal, crown, and lateral roots in maize. *J Exp Bot* 2018;**69**:1199–1206. https://doi.org/10.1093/jxb/erx439

Barrios-Masias F, Knipfer T, McElrone A. Differential responses of grapevine rootstocks to water stress are associated with adjustments in fine root hydraulic physiology and suberization. *J Exp Bot* 2015;**66**:6069–6078. https://doi.org/10.1093/jxb/erv324

Bramley H, Turner NC, Turner DW *et al.* Roles of morphology, anatomy, and aquaporins in determining contrasting hydraulic behavior of roots. *Plant Physiol* 2009;**150**:348–364. https://doi.org/10.1104/pp.108.134098

Brown LK, George TS, Dupuy LX *et al.* A conceptual model of root hair ideotypes for future agricultural environments: what combination of traits should be targeted to cope with limited P availability? *Ann Bot* 2013;**112**:317–330. https://doi.org/10.1093/aob/mcs231

Cai G, Carminati A, Abdalla M *et al.* Soil textures rather than root hairs dominate water uptake and soil–plant hydraulics under drought. *Plant Physiol* 2021;**187**:858–872. https://doi.org/10.1093/plphys/kiab271

Cailloux M. Metabolism and the absorption of water by root hairs. *Can J Bot* 1972;**50**:557–573. https://doi.org/10.1139/b72-069

Caldeira CF, Jeanguenin L, Chaumont F *et al.* Circadian rhythms of hydraulic conductance and growth are enhanced by drought and improve plant performance. *Nat Commun* 2014;**5**:5365. https://doi.org/10.1038/ncomms6365

Carminati A, Moradi AB, Vetterlein D *et al.* Dynamics of soil water content in the rhizosphere. *Plant Soil* 2010;**332**:163–176. https://doi.org/10.1007/s11104-010-0283-8

Carminati A, Passioura JB, Zarebanadkouki M *et al.* Root hairs enable high transpiration rates in drying soils. *New Phytol* 2017;**216**:771–781. https://doi.org/10.1111/nph.2017.216.issue-3

Chaumont F, Tyerman SD. Aquaporins: highly regulated channels controlling plant water relations. *Plant Physiol* 2014;**164**:1600–1618. https://doi.org/10.1104/pp.113.233791

de Willigen P, Heinen M, van Noordwijk M. Roots partially in contact with s solutions and approximation in models of nutrient and water uptake. *Vadose Zone J* 2018;**17**:170060. https://doi.org/10.2136/vzj2017.03.0060

Dodd IC, Diatloff E. Enhanced root growth of the BRB (bald root barley) mutant in drying soil allows similar shoot physiological responses to soil water deficit as wild-type plants. *Funct Plant Biol* 2016;**43**:199. https://doi.org/10.1071/FP15303

Doussan C, Vercambre G, Pagè L. Modelling of the hydraulic architecture of root systems: an integrated approach to water absorption–distribution of axial and radial conductances in maize. *Ann Bot* 1998;**81**:225–232. https://doi.org/10.1006/anbo.1997.0541

Duddek P, Ahmed MA, Javaux M *et al.* The effect of root hairs on root water uptake is determined by root–soil contact and root hair shrinkage. *New Phytol* 2023;**240**:2484–2497. https://doi.org/10.1111/nph.19144

Duddek P, Carminati A, Koebernick N *et al.* The impact of drought-induced root and root hair shrinkage on root–soil contact. *Plant Physiol* 2022;**189**:1232–1236. https://doi.org/10.1093/plphys/kiac144

Duddek P, Papritz A, Ahmed MA *et al.* Observations of root hair patterning in soils: insights from synchrotron-based X-ray computed microtomography. *Plant Soil* 2024;**503**:331–348. https://doi.org/10.1007/s11104-024-06582-1

Enstone DE, Peterson CA, Ma F. Root endodermis and exodermis: structure, function, and responses to the environment. *J Plant Growth Regul* 2002;**21**:335–351. https://doi.org/10.1007/s00344-003-0002-2

Frensch J, Steudle E. Axial and radial hydraulic resistance to roots of maize (*Zea mays* L.). *Plant Physiol* 1989;**91**:719–726. https://doi.org/10.1104/pp.91.2.719

Gambetta GA, Knipfer T, Fricke W *et al. Aquaporins and root water uptake*. In: Chaumont F, Tyerman SD (eds.), *Plant Aquaporins: From Transport to Signaling*. Cham: Springer International Publishing, 2017, 133–153.

Hachez C, Veselov D, Ye Q *et al.* Short-term control of maize cell and root water permeability through plasma membrane aquaporin isoforms. *Plant Cell Environ* 2012;**35**:185–198. https://doi.org/10.1111/j.1365-3040.2011.02429.x

Heymans A, Couvreur V, Lobet G. Combining cross-section images and modeling tools to create high-resolution root system hydraulic atlases in. *Plant Direct* 2021;**5**:e00290. https://doi.org/10.1002/pld3.334

Hinsinger P, Bengough AG, Vetterlein D *et al.* Rhizosphere: biophysics, biogeochemistry and ecological relevance. *Plant Soil* 2009;**321**:117–152. https://doi.org/10.1007/s11104-008-9885-9

Hochholdinger F, Woll K, Sauer M *et al.* Genetic dissection of root formation in maize (*Zea mays*) reveals root-type specific developmental programmes. *Ann Bot* 2004;**93**:359–368. https://doi.org/10.1093/aob/mch056

Hose E, Clarkson D, Steudle E *et al.* The exodermis: a variable apoplastic barrier. *J Exp Bot* 2001;**52**:2245–2264. https://doi.org/10.1093/jexbot/52.365.2245

Itoh S, Barber SA. A numerical solution of whole plant nutrient uptake for soil-root systems with root hairs. *Plant Soil* 1983;**70**:403–413. https://doi.org/10.1007/BF02374895

Javot H, Maurel C. The role of aquaporins in root water uptake. *Ann Bot* 2002;**90**:301–313. https://doi.org/10.1093/aob/mcf199

Kell DB. Breeding crop plants with deep roots: their role in sustainable carbon, nutrient and water sequestration. *Ann Bot* 2011;**108**:407–418. https://doi.org/10.1093/aob/mcr175

Leitner D, Klepsch S, Ptashnyk M *et al.* A dynamic model of nutrient uptake by root hairs. *New Phytol* 2010;**185**:792–802. https://doi.org/10.1111/j.1469-8137.2009.03128.x

Li T, Lin G, Zhang X *et al.* Relative importance of an arbuscular mycorrhizal fungus (*Rhizophagus intraradices*) and root hairs in plant drought tolerance. *Mycorrhiza* 2014;**24**:595–602. https://doi.org/10.1007/s00572-014-0578-3

Lobet G, Couvreur V, Meunier F *et al.* Plant water uptake in drying soils. *Plant Physiol* 2014;**164**:1619–1627. https://doi.org/10.1104/pp.113.233486

Lynch JP. Roots of the second green revolution. *Aust J Bot* 2007;**55**:493–512. https://doi.org/10.1071/BT06118

Lynch JP. Root phenes that reduce the metabolic costs of soil exploration: opportunities for 21st century agriculture. *Plant Cell Environ* 2015;**38**:1775–1784. https://doi.org/10.1111/pce.2015.38.issue-9

Lynch JP. Root phenotypes for improved nutrient capture: an underexploited opportunity for global agriculture. *New Phytol* 2019;**223**:548–564. https://doi.org/10.1111/nph.2019.223.issue-2

Marin M, Feeney DS, Brown LK *et al.* Significance of root hairs for plant performance under contrasting field conditions and water deficit. *Ann Bot* 2021;**128**:1–16. https://doi.org/10.1093/aob/mcaa181

Martre P, North GB, Nobel PS. Hydraulic conductance and mercury-sensitive water transport for roots of *Opuntia acanthocarpa* in relation to soil drying and rewetting. *Plant Physiol* 2001;**126**:352–362. https://doi.org/10.1104/pp.126.1.352

McCully ME, Canny MJ. Pathways and processes of water and nutrient movement in roots. *Plant Soil* 1988;**111**:159–170. https://doi.org/10.1007/BF02139932

Meunier F, Draye X, Vanderborght J *et al.* A hybrid analytical-numerical method for solving water flow equations in root hydraulic architectures. *Appl Math Model* 2017;**52**:648–663. https://doi.org/10.1016/j.apm.2017.08.011

Meunier F, Zarebanadkouki M, Ahmed MA *et al.* Hydraulic conductivity of soil-grown lupine and maize unbranched roots and maize root-shoot junctions. *J Plant Physiol* 2018;**227**:31–44. https://doi.org/10.1016/j.jplph.2017.12.019

North GB, Martre P, Nobel PS. Aquaporins account for variations in hydraulic conductance for metabolically active root regions of agave deserti in wet, dry, and rewetted soil. *Plant Cell Environ* 2004;**27**:219–228. https://doi.org/10.1111/j.1365-3040.2003.01137.x

Palta J, Watt M. *Vigorous crop root systems: form and function for improving the capture of water and nutrients*. San Diego: Academic, 2009, 309–325.

Peterson CA. Exodermal casparian bands: their significance for ion uptake by roots. *Physiol Plant* 1988;**72**:204–208. https://doi.org/10.1111/j.1399-3054.1988.tb06644.x

Peterson RL, Farquhar ML. Root hairs: specialized tubular cells extending root surfaces. *Bot Rev* 1996;**62**:1–40. https://doi.org/10.1007/BF02868919

Robbins NE, Dinneny JR. The divining root: moisture-driven responses of roots at the micro- and macro-scale. *J Exp Bot* 2015;**66**:2145–2154. https://doi.org/10.1093/jxb/eru496

Rosene HF. Quantitative measurement of the velocity of water absorption in individual root hair by a microtechnique. *Plant Physiol* 1943;**18**:588–607. https://doi.org/10.1104/pp.18.4.588

Sanderson J. Water uptake by different regions of the barley root. Pathways of radial flow in relation to development of the endodermis. *J Exp Bot* 1983;**34**:240–253. https://doi.org/10.1093/jxb/34.3.240

Schneider HM, Lynch JP. Functional implications of root cortical senescence for soil resource capture. *Plant Soil* 2018;**423**:13–26. https://doi.org/10.1007/s11104-017-3533-1

Segal E, Kushnir T, Mualem Y *et al.* Water uptake and hydraulics of the root hair rhizosphere. *Vadose Zone J* 2008;**7**:1027–1034. https://doi.org/10.2136/vzj2007.0122

Suzuki N, Taketa S, Ichii M. Morphological and physiological characteristics of a root-hairless mutant in rice (*Oryza sativa* L.). *Plant Soil* 2003;**255**:9–17.

Tripathy KP, Mukherjee S, Mishra AK *et al.* Climate change will accelerate the high-end risk of compound drought and heatwave events. *Proc Natl Acad Sci U S A* 2023;**120**:e2219825120. https://doi.org/10.1073/pnas.2219825120

Vetterlein D, Doussan C. Root age distribution: how does it matter in plant processes? A focus on water uptake. *Plant Soil* 2016;**407**:145–160. https://doi.org/10.1007/s11104-016-2849-6

Vetterlein D, Lippold E, Schreiter S *et al.* Experimental platforms for the investigation of spatiotemporal patterns in the rhizosphere–laboratory and field scale. *J Plant Nutr Soil Sci* 2021;**184**:35–50. https://doi.org/10.1002/jpln.202000079

Wang A, Tao H, Ding G *et al.* Global cropland exposure to extreme compound drought heatwave events under future climate change. *Weather Clim Extrem* 2023;**40**:100559. https://doi.org/10.1016/j.wace.2023.100559

White RG, Kirkegaard JA. The distribution and abundance of wheat roots in a dense, structured subsoil – implications for water uptake. *Plant Cell Environ* 2010;**33**:133–148. https://doi.org/10.1111/j.1365-3040.2009.02059.x

Xiao S, Liu L, Zhang Y *et al.* Fine root and root hair morphology of cotton under drought stress revealed with RhizoPot. *J Agron Crop Sci* 2020;**206**:679–693. https://doi.org/10.1111/jac.12429

Yu P, Li C, Li M *et al.* Seedling root system adaptation to water availability during maize domestication and global expansion. *Nat Genet* 2024;**56**:1245–1256. https://doi.org/10.1038/s41588-024-01761-3

Zhang C, Simpson RJ, Kim CM *et al.* Do longer root hairs improve phosphorus uptake? Testing the hypothesis with transgenic *Brachypodium distachyon* lines overexpressing endogenous RSL genes. *New Phytol* 2018;**217**:1654–1666. https://doi.org/10.1111/nph.14980.

Zimmermann HM, Hartmann K, Schreiber L *et al.* Chemical composition of apoplastic transport barriers in relation to radial hydraulic conductivity of corn roots (*Zea mays* L.). *Planta* 2000;**210**:302–311. https://doi.org/10.1007/PL00008138